



Early gametogenesis in the Pacific oyster: new insights using stem cell and mitotic markers

Patricia Cavelier, Julien Cau, Nathalie Morin, Claude Delsert

► To cite this version:

Patricia Cavelier, Julien Cau, Nathalie Morin, Claude Delsert. Early gametogenesis in the Pacific oyster: new insights using stem cell and mitotic markers. *Journal of Experimental Biology*, 2017, pp.jeb.167734. 10.1242/jeb.167734 . hal-01875258

HAL Id: hal-01875258

<https://hal.science/hal-01875258>

Submitted on 1 Jun 2021

HAL is a multi-disciplinary open access archive for the deposit and dissemination of scientific research documents, whether they are published or not. The documents may come from teaching and research institutions in France or abroad, or from public or private research centers.

L'archive ouverte pluridisciplinaire **HAL**, est destinée au dépôt et à la diffusion de documents scientifiques de niveau recherche, publiés ou non, émanant des établissements d'enseignement et de recherche français ou étrangers, des laboratoires publics ou privés.

RESEARCH ARTICLE

Early gametogenesis in the Pacific oyster: new insights using stem cell and mitotic markers

Patricia Cavelier^{1,2}, Julien Cau^{1,3}, Nathalie Morin^{1,4} and Claude Delsert^{1,4,5,*}

ABSTRACT

While our knowledge of bivalve gametogenesis has progressed in recent times, more molecular markers are needed in order to develop tissue imaging. Here, we identified stem cell and mitotic markers to further characterize oyster early gametogenesis, mainly through immunofluorescence microscopy. Intense alkaline phosphatase activity, a non-specific marker for stem cells, was detected on the outer edge of the gonad ducts at the post-spawning stage, suggesting an abundance of undifferentiated cells very early during the sexual cycle. This observation was confirmed using an antibody against Sox2, a transcription factor specific for stem or germline cells, which labeled cells in the gonad duct inner mass and ciliated epithelium early during the initial oyster sexual cycle. Moreover, Vasa, a cytoplasmic marker for germline cells, was also detected in the gonad acini and duct cells, thus confirming that germline cells were abundant early on. In addition, the binding of the minichromosome maintenance MCM6 protein to chromatin indicated the gonad acini and duct cells were engaged in the cell cycle. DNA replication was indeed confirmed by an abundant *in vivo* incorporation of BrdU into the duct cell chromatin. Finally, proliferation of acini and duct cells was demonstrated by the chromatin-bound Ser10-phosphorylated histone H3, a mitotic marker. The markers for the cell cycle and mitosis used here thus indicate that acini and duct cells were already actively dividing early during the oyster sexual cycle. In addition, together with the stem cell markers, these data reveal that the epithelium delimiting the duct outer edge contains a dynamic population of undifferentiated cells.

KEY WORDS: Germline cells, Cell cycle, Reproduction, Bivalve, Marine invertebrates

INTRODUCTION

Gametogenesis has long been of interest in bivalves (reviewed in Galtsoff, 1964), and has received renewed attention following the development of genomics in bivalves (Fabioux et al., 2004a,b, 2009; Llera-Herrera et al., 2013; Milani et al., 2015, 2017; Obata et al., 2010; Teaniniuraitemoana et al., 2017) and, more recently, because of current environmental concerns (Barranger et al., 2014; Cubero-Leon et al., 2012; de Sousa et al., 2014).

The specification and development of gametes is a central process in animal life cycles in which gametes are derived from primordial germ cells (PGCs) that arise early during embryogenesis and

migrate to the developing gonad. In pre-adult gonads, PGCs become germline stem cells (GSCs) that differentiate into germ cells at sexual maturity (reviewed in Saffman and Lasko, 2009).

GSCs commonly reside in a special microenvironment, termed niche, provided by somatic support cells, in which they both self-renew and produce progeny germ cells that begin the process of differentiation while leaving the niche (reviewed in Spradling et al., 2011). GSCs were originally identified according to their morphology, namely a large round nucleus, a large nucleolus, and a granular cytoplasmic region referred to as the nuage or germ plasm (reviewed in Extavour and Akam, 2003).

Two distinct modes of germline formation have been recognized in animals: epigenesis and preformation (reviewed in Extavour and Akam, 2003; Obata and Komaru, 2012; Spradling et al., 2011; Reitzel et al., 2016). Extavour and Akam (2003) noted that epigenesis occurs in the majority of a series of phyla (23 out of 28), including mammals (Saffman and Lasko, 1999), echinoderms (Juliano et al., 2006) or cnidarians (Noda and Kanai, 1977) in which germ cells are formed later during development under the influence of signals from neighboring cells.

Nevertheless, preformation occurs in many other organisms including *Drosophila*, *Caenorhabditis*, fish teleosts and *Xenopus*, in which germ cells are already present during early embryogenesis. For instance, the cytoplasmic cortical region of the *Xenopus* oocyte vegetal pole that contains an accumulation of mitochondria, granules and specific proteins and RNAs will become the PGC territory after fertilization (Heasman et al., 1984; Kloc et al., 2002; reviewed in Obata and Komaru, 2012). In the Pacific oyster, the PGC specification appears to follow the preformation pattern as the maternally inherited germ plasm is transmitted to specific blastomeres and later, at the gastrula stage, it is distributed at the precursors of the germline (reviewed in Obata and Komura, 2012).

Vasa is an evolutionarily conserved DEAD-box RNA helicase (Castrillon et al., 2000; Extavour et al., 2005; Leininger et al., 2014; Reitzel et al., 2016) that plays different functions in germ cell formation and germline maintenance (reviewed in Lasko, 2013). Fabioux et al. (2004b) confirmed the preformation mode of formation of PGCs through *in situ* hybridization (ISH) on various oyster developmental stages using a *vasa* antisense probe. Indeed, *vasa* RNA was detected on the oocyte vegetal pole and its expression was followed through the 4d cell lineage until a well-defined location was revealed in two clusters of cells, referred to as the germinal primordium, at the veliger stage, 14 days after fertilization. Indeed, *vasa* expression was shown to be necessary to gonad development and maintenance in the oyster (Fabioux et al., 2009). Moreover, Fabioux et al. (2004a) showed that *vasa* is specifically expressed in gonad duct cells during the initiation of the oyster reproductive cycle as well as during later stages of gametogenesis. In addition, cell foci stained for *vasa* expression suggested the presence of GSCs in the mantle during the oyster resting period. Likewise, Obata et al. (2010) identified *vasa*-positive

¹Université de Montpellier, 34095 Montpellier, France. ²IGMM CNRS UMR 5535, 34293 Montpellier, France. ³IGH CNRS UPR 1142, 34396 Montpellier, France.

⁴CRBM CNRS UMR5237, 34293 Montpellier, France. ⁵3AS Ifremer, 34250 Palavas-les-Flots, France.

*Author for correspondence (claude.delsert@crbm.cnrs.fr)

© C.D., 0000-0002-2850-9234

cells in *Mytilus galloprovincialis*, again suggesting the existence of GSCs in connective tissue during the non-reproductive season in mussel. Interestingly, as will be further discussed below, Milani et al. (2015, 2017) confirmed through confocal microscopy that Vasa is a germ cell marker in several species of bivalve.

Oysters are hermaphrodites with an annual alternating rhythm of male and female phases throughout life (Coe, 1931) and their sex determination is influenced by environmental conditions such as temperature, photoperiod and food abundance (Coe, 1936; Fabioux et al., 2005; Santerre et al., 2013). The oyster gonad consists of branching ducts integrated into the connective tissues surrounding the visceral mass that are clearly visible 8–12 weeks after settlement of the spat (reviewed in Galtsoff, 1964).

The stages of oyster gonad development have been defined (Lango-Reynoso et al., 2000; Franco et al., 2008; Steele and Mulcahy, 1999), and in this study we focused on (i) early gametogenesis, during which ducts are elongated and isolated in the connective tissue, and (ii) the post-spawning stage, at which the female gonad contains large, usually elongated, degenerating oocytes.

The oyster gonad is not permanent, and thus the location of GSCs during the resting period and at the beginning of the sexual cycle is not yet completely clear despite recent progress (Fabioux et al., 2004a; Obata et al., 2010; Milani et al., 2015, 2017). Because GSCs are stem cells that perform several rounds of mitotic division before executing germ cell-specific meiosis (reviewed in Spradling et al., 2011), we examined gametogenesis at an early stage of the oyster sexual cycle using molecular markers for stem cells, for DNA replication and for mitosis.

Here, we detected alkaline phosphatase (AP) activity, which is generally considered as indicative of stem cells and germline cells (reviewed in Extavour and Akam, 2003; O'Connor et al., 2008), on the outer edge of gonad ducts at the post-spawning stage. In addition, confocal analysis showed the presence of Sox2, a marker for stem/precursor cells including in *Crassostrea gigas* (Jemaà et al., 2014), inside the gonad ducts but also on their outer edge at the beginning of the first sexual cycle. Moreover, we detected the germline marker Vasa in the gonad duct cells, in agreement with previous reports (Fabioux et al., 2004b; Obata et al., 2010; Milani et al., 2015). Together, these data indicate that germline cells are abundant in the oyster gonad at a very early stage of the reproductive cycle.

Moreover, the presence of the minichromosome maintenance MCM6 protein (O'Donnell and Li, 2016) indicated that duct cells were engaged in the cell cycle. Indeed, an abundant *in vivo* incorporation of BrdU confirmed the occurrence of DNA replication in gonad ducts. Finally, the phosphorylated state of histone H3 on serine 10 (H3P) revealed numerous ongoing mitoses in the ducts at this early sexual stage.

These new insights into oyster early gametogenesis are discussed in the context of a new hypothesis about the origin of GSCs in adult bivalves (Milani et al., 2015, 2017).

MATERIALS AND METHODS

Animals

Diploid oysters, *Crassostrea gigas* (Thunberg 1793), were bred and reared at the Ifremer experimental facility in Bourgneuf bay (Bouin, France), unless otherwise specified. Genitor and experimental animal ploidy level were determined by fluorescence-activated cell sorting (FACS) on gill tissue samples as previously described (Barranger et al., 2014; Jemaà et al., 2014). Oysters were maintained in large tanks with flowing seawater and fed *ad libitum* at the Ifremer Mediterranean facility (Palavas-les-Flots, France).

Histochemistry and immunohistochemistry

Tissues were fixed using Davidson's fixative (for 1 l: 330 ml 95% ethyl alcohol, 220 ml 37% formaldehyde solution, 115 ml glacial acetic acid, 335 ml filtered seawater, FSW) at 4°C for 16 h. Tissue samples were then dehydrated in 70%, 80% and 96% successive ethanol baths and then twice in xylene before embedding in paraffin. Cross-sections (5 µm thick) were cut using an HM355S microtome (Thermo Scientific, Illkirch, France) and then dried overnight at 37°C. For histology, tissue slides were incubated with hematoxylin for 2 min and then counterstained for 4 min with eosin G (0.5% ethanol), and washed in 100% ethanol and xylene before mounting in Mountex medium (Histolab, Seoul, Korea).

For immunohistochemistry (IHC), sections were incubated with primary antibodies diluted in 2% bovine serum albumin in Tris-buffered saline-Tween (TBST) overnight in a humid chamber at 4°C.

Histochemistry

For alkaline phosphatase activity, 1 cm-thick oyster transverse sections were incubated in 4% PFA (EMS, Hatfield, USA) in FSW for 4 h at room temperature. Tissues were rinsed in FSW and then successively incubated for 1.5 h at room temperature in 10% and 20% sucrose in FSW before an overnight incubation at 4°C in 30% sucrose in FSW. Tissue sections were embedded in OCT (Finetek, Chicago, IL, USA) and then frozen on dry ice and conserved at –80°C. Subsequently, 30 µm-thick cryo-sections were post-fixed in 0.5% glutaraldehyde in phosphate-buffered saline (PBS) for 15 min and then rinsed in a large excess of PBS twice for 1 h at room temperature. Sections were then rinsed in buffer B (0.15 mol l⁻¹ NaCl, 0.1 mol l⁻¹ Tris, 50 mmol l⁻¹ MgCl₂, pH 9.5) for 15 min and then incubated in the dark in Purple Blue reagent (Merck Millipore, Darmstadt, Germany) at room temperature. Sections were mounted using Mowiol mounting medium and images were acquired through bright-field microscopy (Leica, Wetzlar, Germany).

Antibodies

The following antibodies were used: monoclonal anti-BrdU (B-8434, IgG1, Sigma-Aldrich, St Louis, MO, USA) at 1/500 dilution; rabbit polyclonal anti-phosphorylated histone H3 (H3P; 06-570, immunopurified; Merck Millipore) at 1/1000 dilution; rabbit polyclonal anti-Sox2 (ab97959, immunopurified; Abcam, Cambridge, MA, USA) at 1/1000 dilution; rabbit polyclonal anti-Vasa (Ab209710, Abcam) at 1/300 dilution; and immunopurified rabbit antibody raised against the recombinant MCM6 protein of *X. laevis* (BAP63987.1) at 1/300 dilution (kind gift of Dr D. Fisher, IGMM, Montpellier, France) (Sible et al., 1998).

BrdU incorporation

A 100 µl volume of 1.6 mmol l⁻¹ BrdU solution was injected into the sinus of the adductor muscle of oysters (1.8 g of meat, *n*=3), which were maintained in FSW at room temperature for 24 h before fixation of the entire body.

Microscopy

Images were viewed using a Zeiss Axioimager Z2 (Oberkochen, Germany) with a Zeiss 20× Plan Apo 0.8 and Zeiss 40× Plan Apo 1.3 Oil DIC (UV) VIS-IR. IHC fluorescence micrographs were collected using a Coolsnap HQ2 CCD camera (Roper Scientific, Evry, France). Bright-field images for histology and histochemistry were collected using a Coolsnap Cf camera (Roper Scientific, Evry, France). Both cameras were driven by Metamorph 7.1 software (Molecular Devices, Sunnyvale, CA, USA). Confocal microscopy was performed using a Zeiss LSM780 confocal microscope with a

Zeiss 40× PLAN APO 1.3 oil DIC (UV) VIS-IR. Series of optical sections were collected.

Chromatin extraction and immunoblotting

Tissues were frozen in liquid nitrogen, pulverized in a press and homogenized using a tissue homogenizer in modified RIPA buffer (25 mmol l⁻¹ Tris HCl, pH 7.4, 150 mmol l⁻¹ NaCl, 5 mmol l⁻¹ EDTA, 1% Triton, 10% glycerol, 50 mmol l⁻¹ NaF and 10 mmol l⁻¹ sodium glycerophosphate) to which the following were added before use: 2 mmol l⁻¹ dithiothreitol, 1 mmol l⁻¹ Na₃VO₄, protease inhibitor cocktail, 1 mmol l⁻¹ phenyl methyl sulfonyl fluoride (PMSF) and 1 mmol l⁻¹ benzamidine (diluted from fresh stock in isopropanol). All steps were carried out at 0°C. The extract was clarified at low speed for 5 min and the resulting supernatant was centrifuged at 10,000 *g* for 30 min in an SS34 rotor (ThermoFisher Scientific, Waltham, MA, USA). Aliquots of the supernatant were frozen at -80°C for control. The pellet was submitted to sonication (Branson 450D, Danbury, CT, USA) until resuspension. The extract was then subjected to several rounds in a French pressure cell press in order to further homogenize the oyster chromatin. The protein concentration of the chromatin extract was determined using the Bradford assay. Chromatin fractions were frozen at -80°C until further use. Chromatin samples were incubated in Laemmli buffer containing 50 mmol l⁻¹ iodoacetate and again subjected to sonication before heating at 94°C for 10 min. Samples were used for 10% SDS-PAGE and transferred to PVDF membrane (Merck Millipore).

RESULTS

AP activity in the spent oyster gonad

AP activity is commonly used to identify stem and germline cells (reviewed in O'Connor et al., 2008; Štefková et al., 2015). Among the four AP genes present in human and mouse, one particular AP (GCAP) (Millan and Manes, 1988) is specific to the germ cells, in which it is highly expressed and very active (reviewed in Extavour and Akam, 2003).

Interestingly, an oyster protein sequence (XP_011446037) shares significant homology with the human GCAP (P10696), suggesting these genes are orthologous (Fig. S1A). A protocol was adapted to preserve the endogenous AP activity in processed tissues of 18 month old oysters (*n*=3) at the post-spawning stage as ascertained by the presence of degenerating oocytes (Fig. 1). Histochemistry revealed a strong AP activity concentrated on the duct outer edge of the spent gonad, while essentially no activity was detected in the mantle or on the duct inner edge (Fig. 1A). Similarly, AP activity was intense around acini in the connective tissue of the

spent gonad (Fig. 1B). As previously reported (Bevelander, 1952; Eble and Scro, 1996), AP activity was also detected in other oyster tissues such as the mantle epithelium (Fig. S2A) or the digestive ducts (Fig. S2B), but was not in the inner part of the mantle or the digestive gland connective tissue.

The intensity of AP activity and its specific location at the gonad duct outer edge suggest that undifferentiated cells were abundant in the gonad at the very end of the oyster sexual cycle.

Sox2, a stem cell marker in the gonad duct cells early during the sexual cycle

Gonad histology of 8 month old oysters (*n*=3), using hematoxylin and eosin staining, revealed small acini and thin ducts in the connective tissue surrounding the visceral mass (Fig. S3A). At higher magnification, large nuclei with perinuclear chromatin and a large nucleolus (Fig. S3B) indicated the presence of gonias (Franco et al., 2008; Nuurai et al., 2016; Yurchenko and Vaschenko, 2010) in the duct inner cell mass. These observations are in agreement with the young oysters being at stage 1 of gametogenesis (developing-early active) according to Steele and Mulcahy (1999).

IHC was performed using an anti-Sox2 antibody, previously used to reveal oyster stem and/or precursor cells (Jemaà et al., 2014), and the intercalating agent DAPI. Confocal images of DAPI staining inside the gonad ducts revealed large round nuclei with a condensed peripheral chromatin (Fig. 2A,C) typical of gonias, as described above. In addition, the inner cell mass contained a second type of nucleus with condensed chromatin (Fig. 2C), indicative of pro-metaphase.

Surprisingly, both types of nuclei inside the ducts labeled for Sox2 while signal specificity was attested by the absence of labeling of surrounding nuclei, in particular in the connective tissue (Fig. 2A, C) and in the negative controls (Fig. 2B). Together, these data indicate that Sox2, a transcription factor expressed in stem or precursor cells, covers the chromatin of oyster gonias.

Interestingly, some nuclei on the duct outer edge were labeled for Sox2 (Fig. 2A,C), whereas this region has generally been described as a ciliated epithelium, based upon histology (Galtsoff, 1964; Eble and Scro, 1996; Franco et al., 2008). Indeed, the presence of ciliated cells was here confirmed by confocal imaging of IHC (Fig. 3) using anti-polyglutamylated tubulin antibody (Bobinnec et al., 1998) that notably labels cilia (Pathak et al., 2007).

The Sox2-labeled nuclei were elongated, with a rather homogeneous chromatin, and they were not distinguishable from adjacent nuclei that were clearly negative for Sox2 (Fig. 2A,C). Therefore, the Sox2-labeled nuclei in the duct outer edge indicate

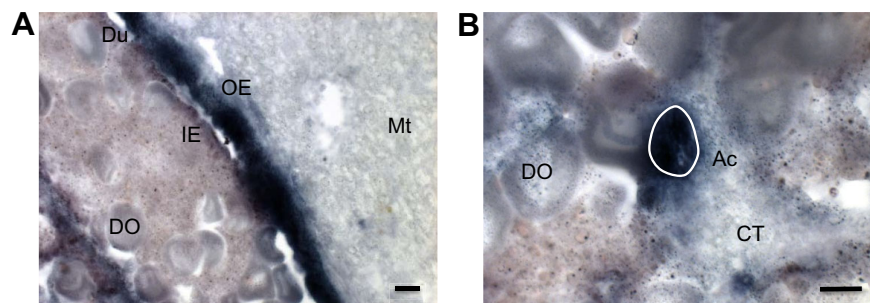


Fig. 1. Alkaline phosphatase (AP) activity in the oyster spent gonad. AP activity in gonad sections of an 18 month old oyster processed after spawning. (A) Intense AP activity is displayed at the outer edge (OE) of the gonad duct (Du) while essentially no AP activity is detected on the duct inner edge (IE) or in the mantle (Mt) or in the resorbing gonad (light-brown) containing degenerating oocytes (DO). (B) Gonad tissues displaying AP activity in acini (Ac, white outline) while little or no activity is detected in the surrounding connective tissue (CT). The large degenerating oocytes (DO) scattered in the gonad tissues are indicative of the post-spawning stage. Scale bars, 100 μ m.

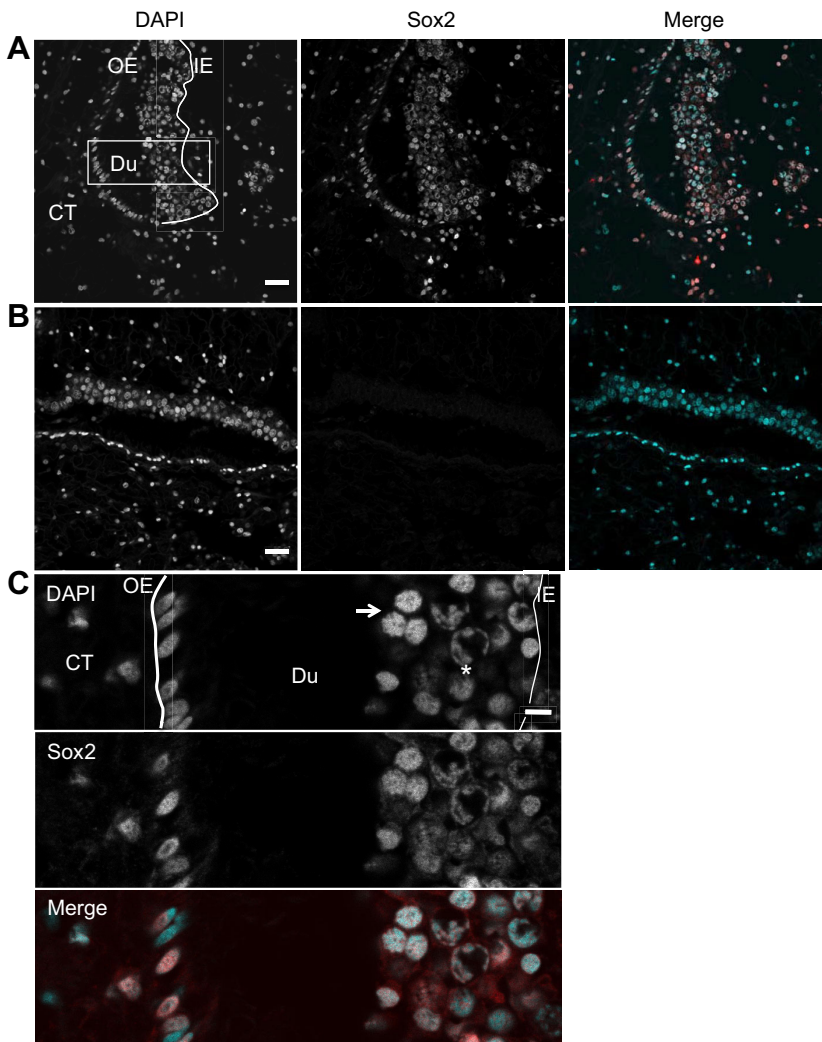


Fig. 2. Sox2 expression in the gonad ducts and acini early during the sexual cycle. Sections of 8 month old oysters were subjected to immunohistochemistry (IHC) using anti-Sox2 antibody and a fluorescent secondary antibody, and DAPI. (A) Confocal image showing Sox2-positive cells both on the duct outer edge (OE) and in the duct (Du) inner cell mass delimited by the inner edge (IE, white line). A few Sox2-positive cells are also scattered in the surrounding connective tissue (CT). Scale bar, 20 µm. (B) Confocal section of a control with no primary antibody. Scale bar, 20 µm. (C) Observation of the duct section in A (boxed region) at higher magnification. DAPI staining shows that the duct inner cell mass delimited by the inner (IE, thin white line) and outer (thick white line) edges contain (i) large nuclei with peripheral chromatin (asterisk) that correspond to gonia as shown through histology (Franco et al., 2008; see Fig. S3) and (ii) groups of smaller nuclei (arrows) with a more condensed chromatin, correspond to pro-metaphase nuclei. Most nuclei in the duct inner cell mass are labeled for Sox2. The duct outer edge is made up of cells with oblong nuclei containing a homogeneous chromatin (DAPI); some of them also labeled for Sox2. Scale bar, 5 µm.

that undifferentiated cells are interspersed among the ciliated epithelial cells, suggesting they are involved in the AP activity detected above (Fig. 1).

Vasa, a germline marker in the duct inner cell mass

To further investigate the nature of the gonad duct cells, we used Vasa, a conserved DEAD-box RNA-dependent helicase, as a marker for the bivalve germline, as previously evidenced by several reports (Fabioux et al., 2004b; Obata et al., 2010; Milani et al., 2015).

A commercial antibody raised against the central domain of the zebrafish Vasa protein (AAI29276.1), which is conserved with its oyster counterpart (NP_001292258.1) (Fig. S1B), revealed a single band of around 80 kDa on an immunoblot of oyster gonad cytosol

while no signal was detected on the gonad chromatin (Fig. S4A). This electrophoretic migration is in agreement with the predicted molecular mass (79.54 kDa) of the oyster Vasa and with recent data by Milani et al. (2017).

Confocal images from IHC using the anti-Vasa antibody revealed a specific cytoplasmic signal in the cells of the gonad acini and duct inner cell mass (Fig. 4A) while no signal was detected in the surrounding connective tissue or in a negative control (Fig. 4B).

The Vasa cytoplasmic signal in the duct inner cells is actually similar to that observed in the gonads of other metazoans, notably the tilapia fish *Oreochromis niloticus* (Kobayashia et al., 2002) and more recently in clam (Milani et al., 2015).

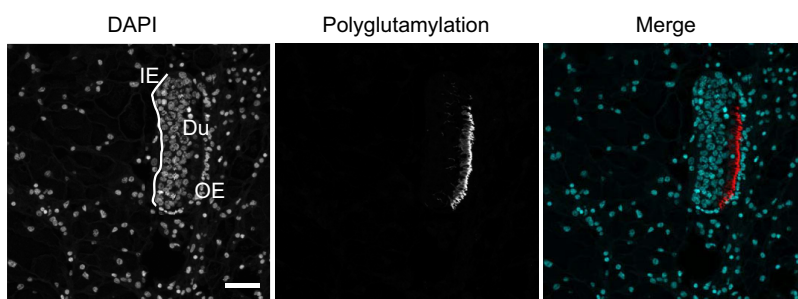


Fig. 3. Polyglutamylated cilia in the gonad duct epithelial cells. IHC was carried out using anti-polyglutamylation antibody and a fluorescent secondary antibody, and DAPI. The confocal section shows the signal for polyglutamylation inside the duct lumina (Du). Thus, the epithelium lining the duct outer edge (OE) indeed contains ciliated cells. IE, duct inner edge (white line). Scale bar, 30 µm.

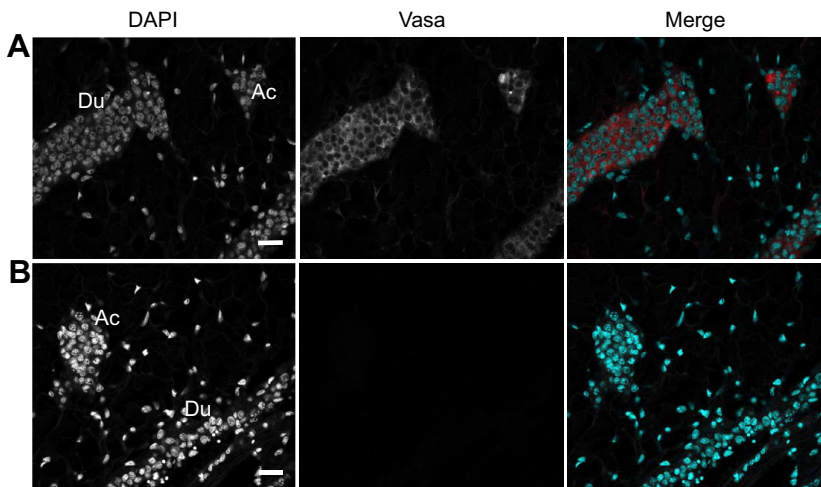


Fig. 4. Vasa expression in the gonad duct inner cell mass. IHC was carried out using anti-Vasa antibody and a fluorescent secondary antibody, and DAPI. (A) Confocal section showing a specific signal for Vasa in the cytoplasm of the gonad duct (Du) and acini (Ac) inner cells. (B) Confocal section of a negative control in the absence of primary antibody. Scale bars, 15 µm.

DNA replication in the gonad at an early stage of the oyster sexual cycle

The minichromosome maintenance MCM6 protein is loaded onto chromatin at replication origins during late mitosis or G1 phase to form pre-replicative complexes (Blow and Dutta, 2005; Hesketh et al., 2015).

MCM6 is conserved through the eukaryotes as illustrated by the homology between mollusk and toad (*X. laevis*) sequences (Fig. S1C). Accordingly, antibody raised against the *Xenopus* MCM6 protein (Sible et al., 1998) revealed a unique band of about 100 kDa on an immunoblot of the chromatin of oyster gonad and gill (Fig. S3B), a tissue known to contain an abundance of proliferating cells (Jemaà et al., 2014). This apparent molecular mass is in good agreement with that of the predicted mollusk MCM6 protein (94 kDa; XP_009061581.1).

Confocal images of IHC performed using the anti-MCM6 antibody revealed an intense signal associated with the DAPI-stained chromatin in the gonad acini, duct inner cell mass and duct ciliated epithelium as well as in a few nuclei in the surrounding connective tissue (Fig. 5A). The specificity of the labeling was shown by fact that nuclei in the mantle connective tissue and in the duct outer edge were not labeled for MCM6 and by the negative control with no primary antibody (Fig. 5C). This result unambiguously indicates that cells in the acini and duct inner mass were engaged in the cell cycle (Namdar and Kearsey, 2006). At higher magnification, groups of nuclei displayed a highly condensed mitotic chromatin corresponding to chromosome individualization during pro-metaphase (Fig. 5B, asterisk).

Interestingly, nuclei in the duct outer edge also labeled for MCM6 (Fig. 5A), which indicates that the duct ciliated epithelium contained cycling cells in addition to the fully differentiated ciliated cells (Fig. 3).

To confirm this observation, oysters ($n=3$) were injected with BrdU, a nucleotide analog, and they were processed 24 h later for IHC as previously described (Jemaà et al., 2014). Confocal images of IHC using a commercial anti-BrdU antibody revealed the typical punctate pattern of BrdU-labeled DNA in the duct inner cells (Fig. 5D). It is noteworthy that BrdU was also incorporated into the cell layer forming the duct outer edge (Fig. 5D), which thus confirms the presence of MCM6 in cells of the epithelial layer (Fig. 5A).

Together, these data show that cells in the duct inner cell mass and in the duct outer edge were engaged in the cell cycle and that DNA replication actually occurred in the gonad duct cells at this early stage of the oyster sexual cycle.

Cell division early during the oyster sexual cycle

Phosphorylation of Ser10 in histone H3 (H3P) is initiated at the late G2 phase during the cell cycle and it lasts throughout different stages of mitosis in eukaryotes (Gurley et al., 1978; Hendzel et al., 1997; Wei et al., 1999).

H3 Ser10 is evolutionarily conserved and, as previously shown, anti-H3P antibody specifically revealed a single band for H3P on an immunoblot of oyster chromatin (Jemaà et al., 2014).

Confocal images of IHC using the anti-H3P antibody revealed an intense signal associated with the DAPI-stained chromatin in the gonad ducts (Fig. 6A) and acini (Fig. 6B) as well as in some nuclei of the surrounding connective tissue. Interestingly, the anti-H3P antibody also labeled nuclei of the duct outer edge epithelium (Fig. 6A), which confirms the findings above for undifferentiated cells (Fig. 2A,C) and for DNA replication (Fig. 5A). Specificity of the H3P signal was confirmed by DAPI-stained nuclei, which were negative for H3P in the surrounding connective tissue, and by the negative control using no primary antibody (Fig. 6C).

This result indicates that the gonad acini and duct inner cells, as well as cells of the duct outer epithelium, were indeed actively engaged in mitosis at this early stage of the oyster sexual cycle.

DISCUSSION

In this study, we used enzymatic activity and antibodies coupled with fluorescence microscopy in order to better characterize the early stage of oyster gametogenesis.

The intense AP activity in the gonad duct outer edge in spent oysters initially drew our attention towards gametogenesis. Indeed, AP activity is a widely accepted marker of stem and germline cells both in culture and within tissues (reviewed in Extavour and Akam, 2003; Štefková et al., 2015). This observation conflicted with the outer edge being only a ciliated epithelium as it has generally been described (reviewed in Galtsoff, 1964; Eble and Scro, 1996). Instead, while the glutamylation of tubulin (Fig. 3) confirmed the presence of terminally differentiated ciliated cells in this epithelium, the intense AP activity displayed by the duct outer edge suggested that, in addition, it contained undifferentiated cells. This hypothesis was indeed supported by the existence of an oyster gene orthologous to human GCAP, a germline-specific gene.

Although other oyster tissues are known to display AP activity, e.g. the mantle epithelium and the digestive tubules, as previously reported (Bevelander, 1952; Eble and Scro, 1996), sections of these tissues used here as controls (Fig. S2) showed in addition that the inner part of the mantle or the connective tissue surrounding the

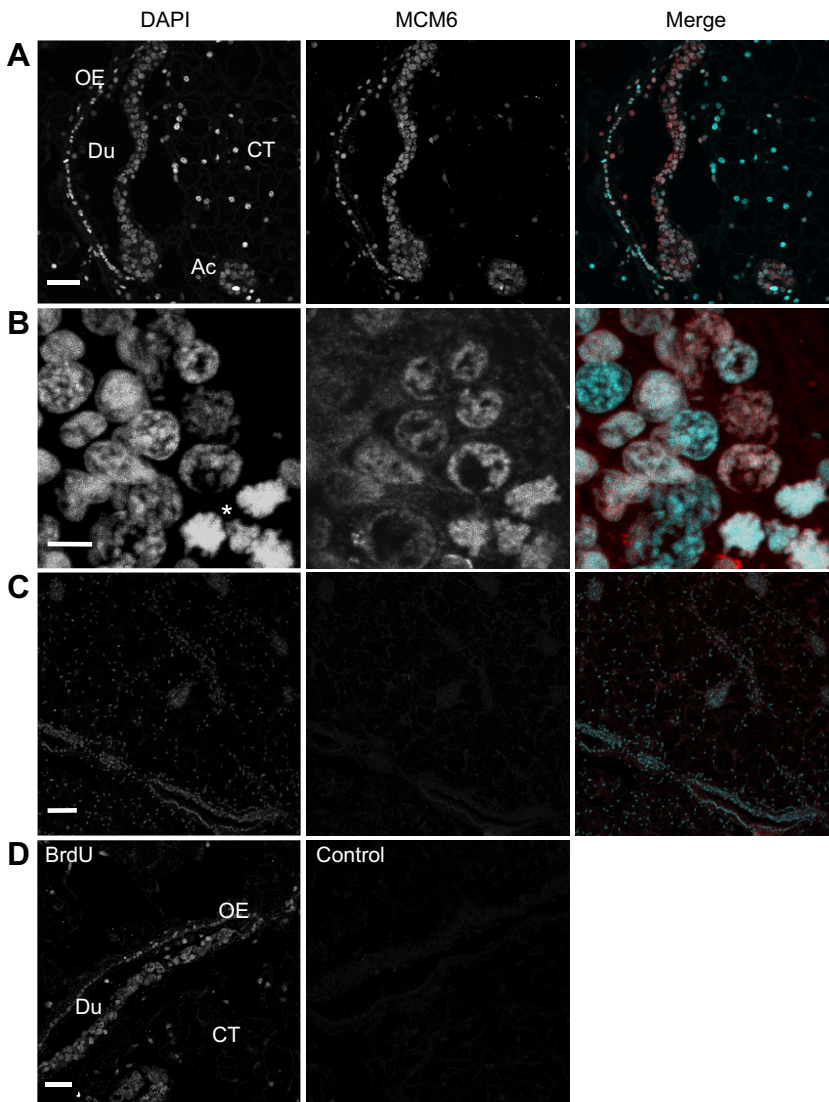


Fig. 5. DNA replication in the gonad duct inner mass and ciliated epithelium. IHC was carried out using anti-MCM6 antibody and a fluorescent secondary antibody, and DAPI. Maximum intensity projections of confocal Z-stacks were acquired through Metamorph. (A) Nuclear signal for MCM6 in gonad duct (Du) and acini (Ac) inner cells and in the epithelium lining the duct outer edge (OE). Cells of the surrounding connective tissue (CT) are mostly negative for MCM6. Scale bar, 20 μ m. (B) Duct inner cell mass at higher magnification, notably showing condensed mitotic chromatin corresponding to pro-metaphase nuclei (asterisk). Scale bar, 10 μ m. (C) Confocal section of a negative control with no primary antibody. Scale bar, 50 μ m. (D) Confocal section of BrdU incorporation into duct cells. IHC carried out using a commercial anti-BrdU antibody revealed a typical dotted BrdU-incorporated chromatin pattern, indicating that DNA replication occurred in the duct (Du) inner cells but also in cells interspersed in the ciliated epithelium forming the duct outer edge (OE) and in a few cells scattered in the surrounding connective tissue (CT). Control with no primary antibody is shown on the right. Scale bar, 20 μ m.

digestive tubules and the gonad ducts displayed comparatively little or no AP activity (Fig. 1; Fig. S2).

The potential diffusion of the AP reaction product could have somehow blurred the exact location of the enzyme. However, the thin and intensely marked region specifically corresponded to the duct outer edge, thus suggesting that the ciliated epithelium contained an abundant population of undifferentiated cells. Moreover, the location of AP activity in the tissue delimiting the gonad duct strongly suggests it was catalyzed by the oyster germline-specific AP gene, at a time when the previous cycle of reproduction was not yet fully completed, as ascertained by the presence of degenerating oocytes (Fig. 1).

To further characterize the early stage of the oyster sexual cycle, we experimented on 8 month old animals, at the beginning of their first reproductive cycle. Histological analysis showed thin gonad ducts with a small inner cell mass in the connective tissue surrounding the oyster visceral mass. At higher magnification, large nuclei with perinuclear chromatin and a large nucleolus showed the presence of gonidia in the duct inner cell mass but also of nuclei with condensed chromatin, which indicated mitotic cells (Fig. S3). These data confirm the early stage of gametogenesis in the 8 month old experimental oysters.

We have previously shown that a commercial anti-Sox2 antibody could reveal oyster stem cells, notably in the hematopoietic lineage

(Jemaà et al., 2014). Here, this anti-sox2 antibody used for IHC revealed nuclear labeling in most of the gonad acini and duct cells. Sox2 is a stem cell-specific transcription factor (Liu and Nonomura, 2016) that was recently shown in proliferating fish gonidia (Patra et al., 2015), a stage of gametogenesis that corresponds to the pattern of chromatin condensation observed in oyster gonad ducts (Fig. 2C) (Franco et al., 2008; Nuurai et al., 2016). Together with the intense AP activity, the presence of Sox2-positive cells interspersed in the duct ciliated epithelium (Fig. 2) unambiguously indicates the presence of stem or precursor cells in this epithelium.

vasa expression is a common marker for germline cells in many animal species, including bivalves (Fabioux et al., 2004a,b; Obata et al., 2010; Milani et al., 2015, 2017), as detailed in the Introduction. Here, *Vasa* was found in the cytoplasm of the oyster acini and duct inner cells (Fig. 4), similar to what has been described for fish (Kobayashi et al., 2002) and clam (Milani et al., 2015). Supporting these findings, *Vasa* expression has been associated with chromatin condensation in *Drosophila* mitotic germ cells (Pek and Kai, 2011).

Interestingly, previous reports have shown the presence of *vasa* RNA in foci of cells in the connective tissue outside the gonad of oyster and mussel (Fabioux et al., 2004b; Obata et al., 2010). More recently, using a mollusk-specific anti-*Vasa* antibody, Milani et al. (2015, 2017) detected *Vasa*-positive cells in or in the vicinity of the

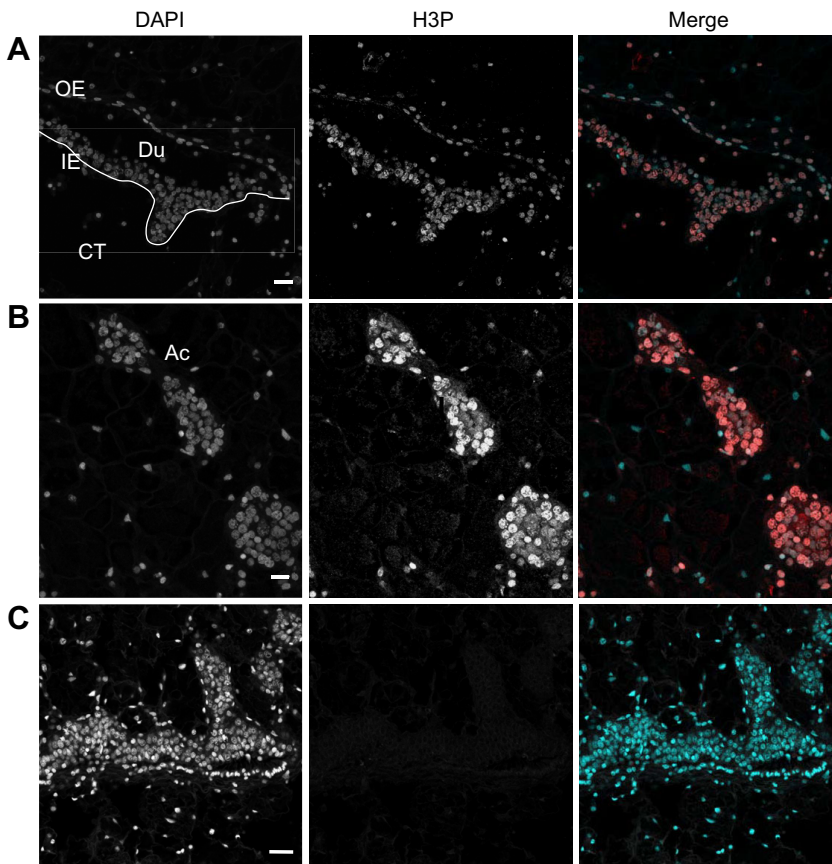


Fig. 6. Mitosis in the gonad duct inner mass and ciliated epithelium. IHC was carried out using a rabbit anti-phosphorylated histone H3 (H3P) antibody and a fluorescent secondary antibody, and DAPI. Maximum intensity projections of confocal Z-stacks were acquired through Metamorph. (A) H3P-positive nuclei are shown in the duct (Du) inner cell mass but also in the epithelium of the outer edge (OE) while neighboring nuclei were not labeled for H3P. A few H3P-positive nuclei are scattered in the connective tissue (CT). IE, duct inner edge (white line). Scale bar, 20 μ m. (B) Higher magnification of acini (Ac) in the gonad tissue displaying H3P-positive nuclei. Scale bar, 10 μ m. (C) Confocal section of a negative control with no primary antibody. Scale bar, 20 μ m.

intestinal epithelium in several bivalves, raising interesting possibilities about the origin of GSCs as discussed below. The fact that, in our experiments, Vasa-positive cells were not observed outside the gonad duct early during oyster gametogenesis might be due to the lack of sensitivity of our antibody, which was raised against fish Vasa.

At maturity, the Pacific oyster gonad accounts for over 30% of body mass, and the production of gametes exceeds 3×10^{11} spermatozooids per male and 5×10^7 oocytes per female (Fabioux, 2004; Suquet et al., 2016), which implies that an intense cell proliferation occurs during gametogenesis.

Proliferation markers would further indicate that the duct inner cell mass contains gonias, as it is the proliferation stage during gametogenesis (reviewed in Spradling et al., 2011), which thus would imply sustained DNA replication. In fact, the MCM6 protein was bound to the chromatin of the oyster duct inner cells but also of cells interspersed in the duct ciliated epithelium (Fig. 5), thus indicating that all these cells were engaged in the cell cycle. Indeed, the MCM complex is loaded onto chromatin at replication origins during late mitosis or G1 phase to form pre-replicative complexes (Blow and Dutta, 2005; Hesketh et al., 2015), and it is absent in quiescent cells (Namdar and Kearsey, 2006). These data were corroborated by the intense incorporation of BrdU into the duct inner cells and in cells of the duct ciliated epithelium. Therefore, the abundance of chromatin-bound MCM6, a replication-associated protein, and the intense BrdU incorporation indicate that DNA was actively replicated in the duct inner cells and in cells of the ciliated epithelium early during the sexual cycle.

Finally, H3P, a mitotic chromosome condensation marker in diverse eukaryotes (Strahl and Allis, 2000; Hans and Dimitrov, 2001), signaled that most of the cells in the duct inner mass as well

as cells in the ciliated epithelium were engaged in mitosis. In fact, cell division was confirmed by groups of pre-metaphase figures in the duct inner cell mass, as shown in Fig. 5B. Together, these data show that an intense cell proliferation occurs early during oyster gametogenesis.

The fact that the gonad duct outer edge contains, in addition to the ciliated epithelial cells, a population of undifferentiated cells that sustains proliferation early during the oyster sexual cycle is most intriguing. This has to be considered in the context of the oyster being a hermaphrodite with an alternating rhythm of male and female phases throughout life, for which a hypothesis about the origin of GSCs in adult tissues has recently been proposed (Obata and Komaru, 2012; Milani et al., 2015, 2017), based notably upon another group of the Lophotrochozoa, the planarians.

Interestingly, germ cells and reproductive structures can be redeveloped *de novo* from neoblasts in planarians after amputation of the entire reproductive system (Morgan, 1901; Wang et al., 2007). As several germ plasm components have been found in planarian neoblasts, Solana (2013) proposed the concept of neoblasts being multipotent stem cells, referred to as primordial stem cells, that can differentiate either in somatic or in germline cells depending upon the context. This concept has recently been proposed by Milani et al. (2017) to explain the presence of Vasa-labeled cells inside or in the vicinity of the gut epithelium in bivalves.

It is noteworthy that the specific regulations governing the self-renewal of stem cells are ill defined outside the vertebrates. In particular, two prominent vertebrate stem cell markers, Oct3/4 and Nanog, are not found in protostomia (Masui, 2011). Identification of more markers for confocal microscopy is therefore a prerequisite for a better understanding of the mechanism pertaining to the protostomia stem cell self-renewal, and this is relevant to the mollusk germline.

Acknowledgements

We are indebted to J. L. Rolland for kindly providing diploid oysters and to D. Fisher for the generous gift of antibodies. We thank B. Chatain (Marbec/Ifremer) and A. Abrieu (CRBM/CNRS) for their support during the course of this work, the members of the CRBM for comments, and the Montpellier RIO Imaging facility for technical support.

Competing interests

The authors declare no competing or financial interests.

Author contributions

Conceptualization: C.D.; Methodology: P.C., J.C., N.M., C.D.; Validation: J.C., N.M., C.D.; Investigation: P.C., C.D.; Supervision: C.D.; Funding acquisition: N.M., C.D.

Funding

This work was supported by a grant of the Ligue Contre Le Cancer to N.M. and by the European Union (grant VIVALDI; H2020 programme, no. 678589) to C.D.

Supplementary information

Supplementary information available online at <http://jeb.biologists.org/lookup/doi/10.1242/jeb.167734.supplemental>

References

- Barranger, A., Akcha, F., Rouxel, J., Brizard, R., Maurouard, E., Pallud, M., Menard, D., Tapie, N., Budzinski, H., Burgeot, T. et al. (2014). Study of genetic damage in the Japanese oyster induced by an environmentally-relevant exposure to diuron: Evidence of vertical transmission of DNA damage. *Aquat. Toxicol.* **146**, 93–104.
- Bevelander, G. (1952). Calcification in molluscs. III. Intake and deposition of Ca^{45} and P^{32} in relation to shell formation. *Biol. Bull.* **94**, 176–183.
- Blow, J. J. and Dutta, A. (2005). Preventing re-replication of chromosomal DNA. *Nat. Rev. Mol. Cell Biol.* **6**, 476–486.
- Bobinac, Y., Moudjou, M., Fouquet, J. P., Desbruyères, E., Eddé, B. and Bornens, M. (1998). Glutamylation of centriole and cytoplasmic tubulin in proliferating non-neuronal cells. *Cell Motil. Cytoskeleton* **39**, 223–232.
- Castrillon, D. H., Quade, B. J., Wang, T. Y., Quigley, C. and Crum, C. P. (2000). The human VASA gene is specifically expressed in the germ cell lineage. *Proc. Natl. Acad. Sci. USA* **97**, 9585–9590.
- Coe, W. R. (1931). Sexual rhythm in the California oyster (*O. lurida*). *Science* **74**, 247–249.
- Coe, W. R. (1936). Environment and sex in the oviparous oyster *Ostrea virginica*. *Biol. Bull.* **71**, 353–359.
- Cubero-Leon, E., Ciocan, C. M., Minier, C. and Rotchell, J. M. (2012). Reference gene selection for qPCR in mussel, *Mytilus edulis*, during gametogenesis and exogenous estrogen exposure. *Environ. Sci. Pollut. Res.* **19**, 2728–2733.
- de Sousa, J. T., Milan, M., Bargelloni, L., Pauletto, M., Matias, D., Joaquim, S., Matias, A. M., Quillien, V., Leitão, A. and Huvet, A. (2014). A microarray-based analysis of gametogenesis in two Portuguese populations of the European clam *Ruditapes decussatus*. *PLoS ONE* **9**, e92202.
- Eble, A. F. and Scro, R. (1996). General anatomy. In *The Eastern Oyster Crassostrea virginica* (ed. V. S. Kennedy R. I. E. Newell and A. F. Eble), pp. 19–73. Trenton, MD: University of Maryland Medical System.
- Extavour, C. G. and Akam, M. (2003). Mechanisms of germ cell specification across the metazoans: epigenesis and preformation. *Development* **130**, 5869–5884.
- Extavour, C. G., Pang, K., Matus, D. Q. and Martindale, M. Q. (2005). *vasa* and *nanos* expression patterns in a sea anemone and the evolution of bilaterian germ cell specification mechanisms. *Evol. Dev.* **7**, 201–215.
- Fabioux, C. (2004). Origine et développement des cellules germinales chez l'huître *Crassostrea gigas*. PhD thesis, Université de Brest, France. Retrieved from www.theses.fr/2004BRES2018.
- Fabioux, C., Pouvreau, S., Leroux, F. L. and Huvet, A. (2004a). The oyster *vasa*-like gene: a specific marker of the germ line in *Crassostrea gigas*. *Biochem. Biophys. Res. Commun.* **315**, 897–904.
- Fabioux, C., Huvet, A., Lelong, C., Robert, R., Pouvreau, S., Daniel, J. Y., Minguant, C. and Le Pennec, M. (2004b). Oyster *vasa*-like gene as a marker of the germline cell development in *Crassostrea gigas*. *Biochem. Biophys. Res. Commun.* **320**, 592–598.
- Fabioux, C., Huvet, A., Le Souche, P., Le Pennec, M. and Pouvreau, S. (2005). Temperature and photoperiod drive *Crassostrea gigas* reproductive internal clock. *Aquaculture* **250**, 458–470.
- Fabioux, C., Corporeau, C., Quillien, V., Favrel, P. and Huvet, A. (2009). *In vivo* RNA interference in oyster- *vasa* silencing inhibits germ cell development. *FEBS J.* **276**, 2566–2573.
- Franco, A., Heude Berthelin, C., Goux, D., Sourdaire, P. and Mathieu, M. (2008). Fine structure of the early stages of spermatogenesis in the Pacific oyster, *Crassostrea gigas*. *Tissue Cell* **40**, 251–260.
- Galtsoff, P. S. (1964). The American oyster, *Crassostrea virginica*. *Fishery Bull.* **64**, 324–353.
- Gurley, L. R., D'Anna, J. A., Barham, S. S., Deaven, L. L. and Tobey, R. A. (1978). Histone phosphorylation and chromatin structure during mitosis in Chinese hamster cells. *Eur. J. Biochem.* **84**, 1–15.
- Hans, F. and Dimitrov, S. (2001). Histone H3 phosphorylation and cell division. *Oncogene* **20**, 3021–3027.
- Heasman, J., Quarmby, J. and Wylie, C. C. (1984). The mitochondrial cloud of *Xenopus* oocytes: the source of germinal granule material. *Dev. Biol.* **105**, 458–469.
- Hendzel, M. J., Wei, Y., Mancini, M. A., Van Hooser, A., Ranalli, T., Brinkley, B. R., Bazett-Jones, D. P. and Allis, C. D. (1997). Mitosis-specific phosphorylation of histone H3 initiates primarily within pericentromeric heterochromatin during G2 and spreads in an ordered fashion coincident with chromosome condensation. *Chromosoma* **106**, 348–360.
- Hesketh, E. L., Knight, J. R. P., Wilson, R. H. C., Chong, J. P. J. and Coverley, D. (2015). Transient association of MCM complex proteins with the nuclear matrix during initiation of mammalian DNA replication. *Cell Cycle* **14**, 333–341.
- Jemaà, M., Morin, N., Cavellier, P., Cau, J., Strub, J. M. and Delsert, C. (2014). Adult somatic progenitor cells and hematopoiesis in oysters. *J. Exp. Biol.* **217**, 3067–3077.
- Juliano, C. E., Veronina, E., Stack, C., Aldrich, M., Cameron, A. R. and Wessel, G. M. (2006). Germ line determinants are not localized early in sea urchin development, but do accumulate in the small micromere lineage. *Dev. Biol.* **300**, 406–415.
- Kloc, M., Dougherty, M. T., Bilinski, S., Chan, A. P., Brey, E., King, M. L., Patrick, C. W., Jr and Etkin, L. D. (2002). Three-dimensional ultrastructural analysis of RNA distribution within germinal granules of *Xenopus*. *Dev. Biol.* **241**, 79–93.
- Kobayashita, T., Kajiura-Kobayashita, H. and Nagaham, Y. (2002). Two isoforms of *vasa* homologs in a teleost fish: their differential expression during germ cell differentiation. *Mech. Dev.* **111**, 167–171.
- Lango-Reynoso, F., Chavez-Villalba, J., Cochard, J.-C. and Le Pennec, M. (2000). Oocyte size, a means to evaluate the gametogenetic development of the Pacific oyster, *Crassostrea gigas*. *Aquaculture* **190**, 183–199.
- Lasko, P. (2013). The DEAD-box helicase Vasa: evidence for a multiplicity of functions in RNA processes and developmental biology. *Biochim. Biophys. Acta* **1829**, 810–816.
- Leininger, S., Adamski, W., Bergum, B., Guder, C., Liu, J., Laplante, M., Brâte, J., Hoffmann, F., Fortunato, S., Jordal, S. et al. (2014). Developmental gene expression provides clues to relationships between sponge and eumetazoan body plans. *Nat. Commun.* **5**, 3905.
- Liu, H. and Nonomura, K.-I. (2016). A wide reprogramming of histone H3 modifications during male meiosis I in rice is dependent on the Argonaute protein MEL1. *J. Cell Sci.* **129**, 3553–3561.
- Llera-Herrera, R., García-Gasca, A., Abreu-Goodger, C., Huvet, A. and Ibarra, A. M. (2013). Identification of male gametogenesis expressed genes from the scallop *Nodipecten subnodosus* by suppressive subtraction hybridization and pyrosequencing. *PLoS ONE* **8**, e73176.
- Masui, S. (2011). Function of Oct3/4 and Sox2 in pluripotency. In *Nuclear Reprogramming and Stem Cells* (ed. J. Ainscough, S. Yamanaka and T. Tada), pp. 117–119. New York: Humana Press. Springer.
- Milani, L., Ghiselli, F., Pecci, A., Maurizii, M. G. and Passamonti, M. (2015). The expression of a novel mitochondrially-encoded gene in gonadic precursors may drive paternal inheritance of mitochondria. *PLoS ONE* **10**, e0137468.
- Milani, L., Pecci, A., Ghiselli, F., Passamonti, M., Bettini, S., Franceschini, V. and Maurizii, M. G. (2017). *Vasa* expression suggests shared germ line dynamics in bivalve molluscs. *Histochem. Cell Biol.* **148**, 157–171.
- Millan, J. L. and Manes, T. (1988). Seminoma-derived Nagao isozyme is encoded by a germ-cell alkaline phosphatase gene. *Proc. Natl. Acad. Sci. USA* **85**, 3024–3028.
- Morgan, T. H. (1901). Morgan TH. Growth and regeneration in *Planaria lugubris*. *Archiv für Entwicklungsmechanik der Organismen*. **13**, 179–212.
- Namdar, M. and Kearsey, S. E. (2006). Analysis of Mcm2–7 chromatin binding during anaphase and in the transition to quiescence in fission yeast. *Exp. Cell Res.* **312**, 3360–3369.
- Noda, K. and Kanai, C. (1977). An ultrastructural observation on *Pelmatothryda robusta* at sexual and asexual stages, with a special reference to "Germinal plasm". *J. Ultrastruct. Res.* **61**, 284–294.
- Nurrai, P., Panasophonkum, S., Tinikul, Y., Sobhon, P. and Wanichanon, R. (2016). Spermatogenesis in the rock oyster, *Saccostrea forskali*. *Tissue Cell* **48**, 43–48.
- Obata, M. and Komaru, A. (2012). The mechanisms of primordial germ cell determination during embryogenesis in molluscan species. *Invert. Surviv. J.* **9**, 223–229.
- Obata, M., Sano, N., Kimata, S., Nagazawa, K., Yoshizaki, G. and Komaru, A. (2010). The proliferation and migration of immature germinal cells in the mussel, *Mytilus galloprovincialis*: observation of the expression pattern in the *vasa*-like gene by *in situ* hybridization. *Dev. Genes* **220**, 139–149.
- O'Connor, M. D., Kadel, M. D., Iosifina, I., Youssef, D., Lu, M., Li, M. M., Vercaute-ren, S., Nagy, A. and Eaves, C. J. (2008). Alkaline phosphatase-

- positive colony formation is a sensitive, specific, and quantitative indicator of undifferentiated human embryonic stem cells. *Stem Cells* **26**, 1109–1116.
- O'Donnell, M. and Li, H. (2016). The eukaryotic replisome goes under the microscope. *Curr. Biol.* **26**, R247–R256.
- Pathak, N., Obara, T., Mangos, S., Liu, Y. and Drummond, I. A. (2007). The zebrafish fleer gene encodes an essential regulator of cilia tubulin polyglutamylation. *Mol. Biol. Cell.* **18**, 4353–4364.
- Patra, S. K., Chakrapani, V., Panda, R. P., Mohapatra, C., Jayasankar, P. and Barman, H. K. (2015). First evidence of molecular characterization of rohu carp Sox2 gene being expressed in proliferating spermatogonial cells. *Theriogenology* **84**, 268–276.
- Pek, J. W. and Kai, T. (2011). A role for Vasa in regulating mitotic chromosome condensation in *Drosophila*. *Curr. Biol.* **21**, 39–44.
- Reitzel, A. M., Pang, K. and Martindale, M. Q. (2016). Developmental expression of “germline”- and “sex determination”-related genes in the ctenophore *Mnemiopsis leidyi*. *Evo. Devo.* **7**, 17.
- Saffman, E. E. and Lasko, P. (1999). Germline development in vertebrates and invertebrates. *Cell. Mol. Life Sci.* **55**, 1141–1163.
- Santerre, C., Sourdain, P., Marc, N., Mingant, C., Robert, R. and Martinez, A.-S. (2013). Oyster sex determination is influenced by temperature- First clues in spat during gonadic differentiation and gametogenesis. *Comp. Bioch. Physiol. A* **165**, 61–69.
- Sible, J. C., Erikson, E., Hendrickson, M., Maller, J. L. and Gautier, J. (1998). Developmental regulation of MCM replication factors in *Xenopus laevis*. *Curr. Biol.* **8**, 347–350.
- Solana, J. (2013). Closing the circle of germline and stem cells: the Primordial Stem Cell hypothesis. *Evo. Devo.* **4**, 2.
- Spradling, A., Fuller, M. T., Braun, R. E. and Yoshida, S. (2011). Germ line stem cells. *Cold Spring Harb. Perspect. Biol.* **3**, 1–20.
- Steele, S. and Mulcahy, M. F. (1999). Gametogenesis of the oyster *Crassostrea gigas* in southern Ireland. *J. Mar. Biol. Assoc. UK* **70**, 673–686.
- Štefková, K., Procházková, J. and Pacherník, J. (2015). Alkaline phosphatase in stem cells. *Stem Cells Int.* **2015**, 628368.
- Strahl, B. D. and Allis, C. D. (2000). The language of covalent histone modifications. *Nature* **403**, 41–45.
- Suquet, M., Malo, F., Quere, C., Leduc, C., Le Grand, J. and Benabdelmouna, A. (2016). Gamete quality in triploid Pacific oyster (*Crassostrea gigas*). *Aquaculture* **451**, 11–15.
- Teaniniuraitemoana, V., Leprêtre, M., Levy, P., Vanaa, V., Parrad, S., Gaertner-Mazouni, N., Gueguen, Y., Huvet, A. and Le Moullac, G. (2016). Effect of temperature, food availability, and estradiol injection on gametogenesis and gender in the pearl oyster *Pinctada margaritifera*. *J. Exp. Zool. A Ecol. Genet. Physiol.* **325**, 13–24.
- Wang, Y., Zayas, R. M., Guo, T. and Newmark, P. A. (2007). nanos function is essential for development and regeneration of planarian germ cells. *Proc. Natl. Acad. Sci. USA* **104**, 5901–5906.
- Wei, Y., Yu, L., Bowen, J., Gorovsky, M. A. and Allis, C. D. (1999). Phosphorylation of histone H3 is required for proper chromosome condensation and segregation. *Cell* **97**, 99–109.
- Yurchenko, O. and Vaschenko, M. A. (2010). Morphology of spermatogenic and accessory cells in the mussel *Modiolus kurilensis* under environmental pollution. *Mar. Env. Res.* **70**, 171–180.

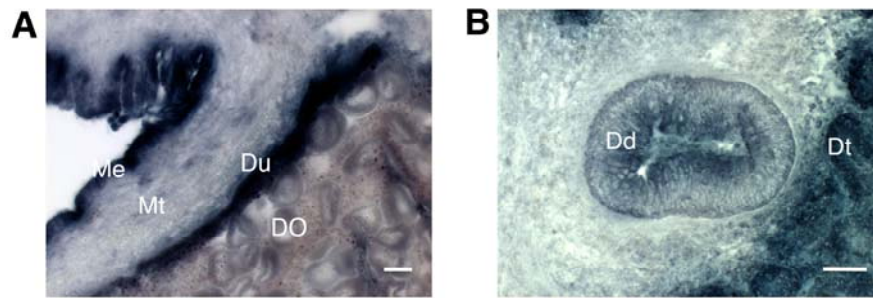
A

B

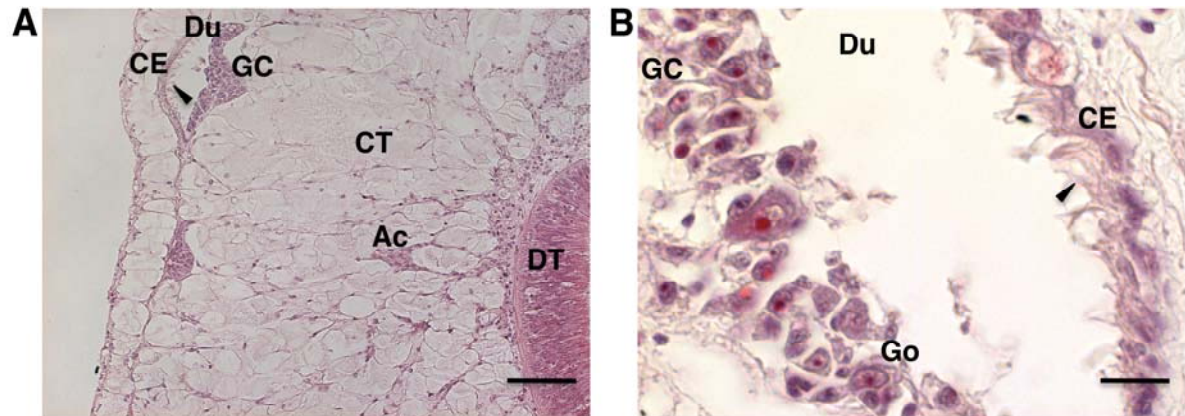
C

C. gigas 1 70 80 90 100 110 120 130 140 150 160 170 180 190 200 210 220 230 240 250 260
L. gigantea MDVAETITVTIKQVQDVGERCQKLFDFLEER-VEGEQKYTAGINDIGPERN
X. laevis MDVAETITQTNQNVQDVGERCQKLFDFLEEAAG-GESESKYLSVEQLIRPERN
C. gigas 70 80 90 100 110 120 130 140 150 160 170 180 190 200 210 220 230 240 250 260
L. gigantea TLTVTSFVQKNGNLLATTILEEYRYVYPFLCRAYNRVKNQAGTQGKEIVSYFTDVTIRLKV
X. laevis TLTVTSFVQKNGNLLATTILEEYRYVYPFLCRAYNRVKNQAGTQGKEIVSYFTDVTIRLKV
C. gigas 140 150 160 170 180 190 200 210 220 230 240 250 260
L. gigantea EMTTAKITGLTRLITGGQVVRTPHPVPELVSGTFLDCRTVMQVDEQFQKIQPTQPTICRNYPVCNNRQ
X. laevis ELSAAKITGLTRLITGGQVVRTPHPVPELVSGTFLCMEQGSIVKQVEQQRITQPTIKCNPVCAANR
C. gigas 270 280 290 300 310 320 330 340 350 360 370 380 390 400 410 420 430 440 450 460 470 480 490 500 510 520 530 540 550 560 570 580 590 600
L. gigantea RFMLDVNKS RFVDFQKVR IQETQAE LPRGSI PRSVEI VLRFAEAVTAAGDGK SDF TGT L VVPDV
X. laevis RFTLBTNKS RFVDFQKVR IQETQAE LPRGSI PRSVEI VLRFAEAVTAAGDGK SDF TGT L VVPDV
C. gigas 270 280 290 300 310 320 330 340 350 360 370 380 390 400 410 420 430 440 450 460 470 480 490 500 510 520 530 540 550 560 570 580 590 600
L. gigantea STIATPQGGVE TGAKV EGGQNGMEGVRGLKALGVRDLTYRLAFLACTVSSNPRFGRRKDEE
X. laevis SALAA-GDARMETGAKVTGEGGNGECVQGLKALGVRDLMLRLALACVGGATNPRGGKRLRE
C. gigas 330 340 350 360 370 380 390 400 410 420 430 440 450 460 470 480 490 500 510 520 530 540 550 560 570 580 590 600
L. gigantea EMTAEIAVKKQMTAEWQVYMSQDNKLQNLCSLPTTHGNEVKRGLLMLFGVGPKTTEG
X. laevis EMTAEIAVKKQMTAEWQVYMSQDNKLQNLCSLPTTHGNEVKRGLLMLFGVGPKTTEG
C. gigas 460 470 480 490 500 510 520 530 540 550 560 570 580 590 600
L. gigantea TNLRGDINIKCVGDPSTAKS QFLQVEFSPRAYVTS GKAS SAAGLTAAVVD E SHEFVIEAG
X. laevis TNLRGDINIKCVGDPSTAKS QFLQVEFSPRAYVTS GKAS SAAGLTAAVVD E SHEFVIEAG
C. gigas 460 470 480 490 500 510 520 530 540 550 560 570 580 590 600
L. gigantea LMLADNGVCCIDEFDPMKDDQVAIHEAQEQTISITKAGVKATLNARTSILAAANPVGGRYDT
X. laevis LMLADNGVCCIDEFDPMKDDQVAIHEAQEQTISITKAGVKATLNARTSILAAANPVGGRYDT
C. gigas 530 540 550 560 570 580 590 600
L. gigantea KSLKKNILSTAPIMSRDFLLVLDCEGNEVDYAIARRIVDLHRSNEESVRYVEDMTYRLF
X. laevis KSLKKNILSTAPIMSRDFLLVLDCEGNEVDYAIARRIVDLHRSNEESVRYVEDMTYRLF
C. gigas 590 600 610 620 630 640 650
L. gigantea ARQFQPKISPDQAEEVLEVKRLQRDGSAGSAWIRITVROLESIMRLSEMARLHDEVDQVQK
X. laevis ARQFQPKISPDQAEEVLEVKRLQRDGSAGSAWIRITVROLESIMRLSEMARLHDEVDQVQK
C. gigas 660 670 680 690 700 710 720
L. gigantea ARQFQPKITKAEEVLEVKRLQRDGSAGSAWIRITVROLESIMRLSEMARLHDEVDQVQK
X. laevis ARQFQPKITKAEEVLEVKRLQRDGSAGSAWIRITVROLESIMRLSEMARLHDEVDQVQK
C. gigas 660 670 680 690 700 710 720
L. gigantea HVKEAFRLNKSIIIRVQPDVLEEEEQEEDMDVEPEQTAEATGPDGDAQ-- PH
X. laevis HVKEAFRLNKSIIIRVQPDVLEEEEQEEDMDVEPEQTAEATGPDGDAQ-- PH
C. gigas 720 730 740 750 760 770 780 790 800 810 820 830 840 850 860 870 880 890 900
L. gigantea KKGKLTVEYKQIANLVLVYRQEEEMNDEPGLRRSLGVGYLKEEISEDAELIKKTK
X. laevis KKGKLTVEYKQIANLVLVYRQEEEMNDEPGLRRSLGVGYLKEEISEDAELIKKTK
C. gigas 790 800 810 820 830 840 850 860 870 880 890 900
L. gigantea NAGLKSSEAKNLSINLLVLQKMEET---EEEDCLTITLVNLLKEMAEITETELILKKR
X. laevis NAGLKSSEAKNLSINLLVLQKMEET---EEEDCLTITLVNLLKEMAEITETELILKKR
C. gigas 790 800 810 820 830 840 850 860 870 880 890 900
L. gigantea IIVEKYIIRLVHDHVLIELTGTQMK---GDD-LVREDEPQVIVPNYVID
X. laevis IIVEKYIIRLVHDHVLIELTGTQMK---GDD-LVREDEPQVIVPNYVID
C. gigas 790 800 810 820 830 840 850 860 870 880 890 900
L. gigantea LIEKYIIRLVHDHVLIELNKLTKMDTGTGDEAAEDILVNPNAAD
X. laevis LIEKYIIRLVHDHVLIELNKLTKMDTGTGDEAAEDILVNPNAAD

Suppl. Fig. S1. Evolutionary conservation of oyster markers. Sequence alignment shows that **A.** The oyster AP (XP_011446037.1) protein is the ortholog of the human germline-specific GCAP (P10696.4). **B.** The oyster (NP_001292258.1) protein is the ortholog of the zebrafish germline-specific Vasa (gb|AAI29276.1) that served to raise the Vasa-antibody used in this work. **C.** The mollusk (XP_009061581.1) protein is the ortholog of the *Xenopus* Minichromosome maintenance MCM6 protein (BAP63987.1) that served to raise the MCM6-antibody used in this work.

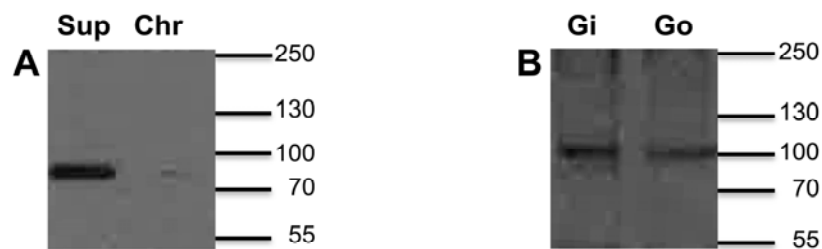


Suppl. Fig. S2. Alkaline Phosphatase activity in spent oyster tissues. A. Mantle. The strong AP activity on the mantle epithelium (Me) is comparable in intensity to the gonad duct (Du) signal, while little activity was detected in the mantle (Mt) and the degenerating oocytes (DO). B. Digestive gland. AP activity was detected in the digestive tubules (Dt) and ducts (Dd) while essentially no AP activity was present in the surrounding connective tissues (CT). Scale bars, 100 μ m.



Suppl. Fig. S3. Oyster gonad histology early during the sexual cycle. Hematoxylin- and eosin-stained sections of 8-month-old oysters. **A.** Gonad duct (Du) and acini (Ac) are shown in the connective tissues (CT) surrounding the oyster visceral mass. Germ cells (GC) are visible on the inner edge of the duct while the outer edge is constituted of an epithelium (CE) displaying cilia (arrow head) in the duct lumina. Thinness of the ducts that are only partially filled with germ cells confirmed that the experimental oysters were at an early stage of their sexual cycle (Steele and Mulcahy, 1999; Lango-Reynoso et al., 2000). DT, digestive tube. Scale bar, 100 μ m.

B. Detail of a duct section at higher magnification showing germ cell (GC) cluster containing gonion (Go) with a large nucleus containing perinuclear chromatin and a large nucleolus (Franco et al., 2008; Nuurai et al., 2016). Epithelium (CE) harboring cilia (arrow head) delimits the duct outer edge. Scale bar, 10 μ m.



Suppl. Fig. S4. Antibody specificity for oyster proteins. Immunoblots were carried out against oyster chromatin (A and B) or cytosolic extract (A) (50 μ g and 10 μ g of total proteins, respectively) transferred to PVDF membrane. (A) A commercial Vasa rabbit antibody raised against the central domain (AA 199 to 526) of the *Xenopus laevis* Vasa revealed a unique band (81 kDa) of the oyster Vasa (EKC30448.1) predicted molecular weight on gonad cytosolic extract (Sup) while no band was detected on gonad chromatin (Chr). (B) MCM6 rabbit antibody (Sible et al., 1998) revealed a unique band (93 kDa) of the mollusk MCM6 (XP_009061581) predicted molecular weight on the chromatin of gill (Gi) and gonad (Go). PageRuler marker in kDa.